

Optical consequences of long-range order in wurtzite $\text{Al}_x\text{Ga}_{1-x}\text{N}$ alloys

S. V. Dudiy and Alex Zunger

National Renewable Energy Laboratory, Golden, Colorado 80401, USA

(Received 22 April 2003; published 9 July 2003)

The effect of 1:1 long range order on optical properties of $\text{Al}_x\text{Ga}_{1-x}\text{N}$ alloys is investigated by means of first-principles calculations combined with large-scale atomistic empirical-pseudopotential simulations. We propose an intra-band mechanism of ordering-induced band gap reduction for different optical polarization. The scaling of band gap reductions with order parameter is analyzed. Our simulations of inhomogeneous ordering suggest that coexistence of ordered and random domains may explain the large magnitude of the observed redshifts upon ordering.

DOI: 10.1103/PhysRevB.68.041302

PACS number(s): 78.20.Bh, 71.55.Eq, 71.20.Nr, 71.70.-d

Spontaneous CuPt ordering of otherwise random *zincblende* III-V semiconductor alloys¹ (e.g., $\text{Ga}_x\text{In}_{1-x}\text{P}$) results in doubling of the unit cell into an alternate monolayer superlattice $(\text{GaP})_1/(\text{InP})_1$. This cell doubling folds *non- Γ* bands onto the Brillouin zone center, creating new optical transitions due to such inter-valley (e.g., Γ -L) coupling. The recent discovery of 1:1 long-range ordering in *wurtzite* III-V nitride alloys AlGaN_2 (Ref. 2) and $\text{In}_x\text{Ga}_{1-x}\text{N}$ (Ref. 3) brings a new aspect into ordering, as here the cell size does not increase upon ordering, so only intra-band (Γ - Γ) coupling exists. In this Rapid Communication we (i) explain the intra-valley mechanism of band formation for wurtzite ordering, (ii) show that large (~ 1 eV) ordering-induced band gap reduction will not occur in $\text{Al}_x\text{Ga}_{1-x}\text{N}$, unlike what might be expected from extrapolating the currently measured gap reduction to full ordering, and (iii) suggest that the coexistence of ordered with random domains in alloy samples may explain the observed large ordering-induced red shifts.

Depending on the growth method and conditions, a number of different types of long-range ordering in $\text{Al}_x\text{Ga}_{1-x}\text{N}$ alloys can occur.²⁻⁷ The 1:1 type of ordering² is most commonly occurring, even in the presence of other chemically ordered structures in the same sample.⁵⁻⁷ Here we choose to focus on the 1:1 ordering,² in which the cell size does not increase. This allows us to isolate the unusual inter-valley mechanism of band formation from the better known band folding in larger period supercells.

In contrast with the zinc-blend structure, the wurtzite structure (space group $P6_3m1$) has two cation sites per unit cell, T_1 and T_2 . In a perfectly random $\text{Al}_x\text{Ga}_{1-x}\text{N}$ alloy there is equal probability to find an Al or Ga atom on either of these sites. In the ordered alloy the probability for Al atoms to be on the T_1 sites, P_1^{Al} , is different from that on the T_2 sites, P_2^{Al} :

$$P_1^{\text{Al}} = x + \eta/2, \quad P_2^{\text{Al}} = x - \eta/2, \quad (1)$$

where $\eta = |P_1^{\text{Al}} - P_2^{\text{Al}}|$ is the long-range order parameter, $0 \leq \eta \leq 2x$, being 0 for random and 1 for perfectly ordered $\text{Al}_{0.5}\text{Ga}_{0.5}\text{N}$. The space group symmetry is now $P3m1$.

Although the experimental information⁸⁻¹⁰ on how ordering affects $\text{Al}_x\text{Ga}_{1-x}\text{N}$ optical properties is still quite limited, there are indications that partial ordering ($\eta \sim 0.3-0.6$) reduces the band gap of $\text{Al}_x\text{Ga}_{1-x}\text{N}$ alloys by up to a few

tenths of eV.⁸⁻¹⁰ Based on general theoretical considerations,¹¹ the band gap reduction $\Delta E_g(\eta)$ of homogeneous solids scales principally as η^2 . Thus, from extrapolation of currently observed band gap reduction from partial to complete ordering we can expect the band gap reduction at full order, $\Delta E_g(\eta \approx 1)$, to be of the order of 1 eV. This potentially very large band gap reduction raises a number of important questions. In particular, what is the magnitude and origin of ordering-induced band gap reduction, as well as how does $\Delta E_g(\eta)$ scale with η and what can break those scaling laws? In this Rapid Communication we answer those questions using predictive theoretical methods.

(i) *The origin and magnitude of the band gap reduction for completely ordered AlGaN_2* : In the band structure of wurtzite AlN or GaN, the top of the valence band at the Γ point is split by the crystal field into singly degenerate Γ_{1v} and doubly degenerate Γ_{5v} states (Fig. 1, using nonrelativistic notations). The Γ_{1v} state has p_z character [with the z

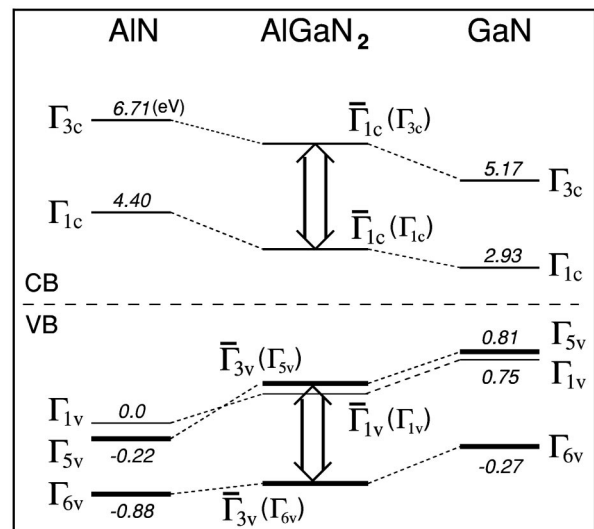


FIG. 1. Schematic diagram showing different symmetry states of the valence (VB) and conduction (CB) bands of AlN and GaN mapping onto same symmetry states of the perfectly ordered AlGaN_2 phase. The numbers represent LDA-calculated eigenvalues, taking into account the LDA-calculated AlN/GaN valence band offset (Ref. 30).

axis along (0001)], whereas the Γ_{5v} states have $p_{x,y}$ character.^{12,13} The different character of these valence states results in two different types of optical transitions at threshold: the xy -polarized $\Gamma_{1c} \leftrightarrow \Gamma_{5v}$ and the z -polarized $\Gamma_{1c} \leftrightarrow \Gamma_{1v}$, with different transition energies, $E_g^{(xy)}$ and $E_g^{(z)}$, respectively. Upon long-range ordering, the Γ_{1v} state of the wurtzite constituents AlN and GaN form the $\bar{\Gamma}_{1v}(\Gamma_{1v})$ state of ordered AlGa_{0.5}N₂, whereas the Γ_{5v} state of the wurtzite constituents form the $\bar{\Gamma}_{3v}(\Gamma_{5v})$ state of AlGa_{0.5}N₂ (we denote states of the ordered compound by bar, and indicate its parenthesis in parentheses). The wurtzite structure also has a deeper valence state of Γ_{6v} symmetry (Fig. 1). This state creates upon ordering another $\bar{\Gamma}_{3v}(\Gamma_{6v})$ state. We see that valence band states of different symmetries (Γ_6 and Γ_5) in the constituent compounds have now formed states of the same symmetry— $\bar{\Gamma}_{3v}(\Gamma_{5v})$ and $\bar{\Gamma}_{3v}(\Gamma_{6v})$ —in the ordered alloy. These states must now repel each other (“avoided crossing”), thus displacing the valence $\bar{\Gamma}_{3v}(\Gamma_{5v})$ state upwards. Figure 1 also shows that the Γ_{1c} and Γ_{3c} conduction states of the wurtzite constituents create, upon ordering, the equal-symmetry states $\bar{\Gamma}_{1c}(\Gamma_{1c})$ and $\bar{\Gamma}_{1c}(\Gamma_{3c})$. Such states must also repel each other, lowering the conduction band minimum (CBM). Thus, upon ordering, the upward shift of $\bar{\Gamma}_{3v}(\Gamma_{5v})$ will reduce the $\bar{\Gamma}_{3v} - \bar{\Gamma}_{1c}$ band gap, while the downward shift of $\bar{\Gamma}_{1c}(\Gamma_{1c})$ will reduce both the $E_g^{(xy)} = \bar{\Gamma}_{3v} - \bar{\Gamma}_{1c}$ and the $E_g^{(z)} = \bar{\Gamma}_{1v} - \bar{\Gamma}_{1c}$ gaps.

To evaluate the magnitude of the ordering-induced band gap reductions for Al_{0.5}Ga_{0.5}N alloy, we perform first-principles calculations for AlN, GaN, ordered AlGa_{0.5}N₂, and random Al_{0.5}Ga_{0.5}N modeled by special quasirandom structures (SQS),¹⁴ using 16 and 32 atom supercells (SQS8 and SQS16).^{14,15} We use the local-density approximation (LDA) (Ref. 16) for the exchange-correlation potential. The calculations are done with the VASP plane-wave pseudopotential code,¹⁷ using projector augmented wave (PAW) potentials.¹⁸ The Ga- d orbitals are included in the valence states. A 500 eV plane wave cutoff is used. The density of the k -point samplings is chosen to be close to that with 40 irreducible k points for a four-atom unit cell of wurtzite AlN or GaN. The lattice constant and c/a -ratio of the random alloy are fixed to the averages of the optimized AlN and GaN values, while allowing relaxation of all cell-internal atomic positions. All the structural parameters of the ordered phase are fully optimized. We do not include the small [≤ 20 meV for GaN and AlN (Ref. 29)] spin-orbit interaction. The LDA calculated maximal ordering-induced band gap reductions for Al_{0.5}Ga_{0.5}N are $\Delta E_g^{(xy)} = 0.17$ and $\Delta E_g^{(z)} = -0.02$ eV, while for unpolarized light, where $E_g = \min\{E_g^{(xy)}, E_g^{(z)}\}$, the reduction is $\Delta E_g = 0.09$ eV (see, however, modified values in Fig. 2 below). Here the band gap reductions are defined as the differences between the optical transition energies of the perfectly ordered and perfectly random systems.

As Fig. 1 shows, in AlN the lowest-energy interband transition is the z -polarized $\Gamma_{1v} \leftrightarrow \Gamma_{1c}$, whereas in GaN it is the xy -polarized $\Gamma_{5v} \leftrightarrow \Gamma_{1c}$.^{12,13} We find that the random alloy at $x = 0.5$ has a z -polarized transition, akin to AlN. Upon ordering of Al_{0.5}Ga_{0.5}N, the $\bar{\Gamma}_{3v}(\Gamma_{5v})$ state is repelled upward [by

the lower $\bar{\Gamma}_{3v}(\Gamma_{6v})$ state], whereas the $\bar{\Gamma}_{1v}(\Gamma_{1v})$ state is not, because there is no other near-lying state of the same symmetry. Thus, ordering changes significantly the crystal field splitting, $\bar{\Gamma}_{3v}(\Gamma_{5v}) - \bar{\Gamma}_{1v}(\Gamma_{1v})$, from -77 meV in random alloy to $+113$ meV in the ordered one. By changing the sign of the crystal field splitting, ordering also changes the polarization of the principal optical transition from z -polarized $\bar{\Gamma}_{1v}(\Gamma_{1v}) \leftrightarrow \bar{\Gamma}_{1c}(\Gamma_{1c})$ in the random alloy to xy -polarized $\bar{\Gamma}_{3v}(\Gamma_{5v}) \leftrightarrow \bar{\Gamma}_{1c}(\Gamma_{1c})$ in the ordered one. The $\Gamma_{5v} - \Gamma_{6v}$ energy difference of 0.93 eV in the random alloy transforms into a 0.2 eV larger $\bar{\Gamma}_{3v} - \bar{\Gamma}_{3v} = 1.13$ eV energy difference in the ordered case. Similarly, ordering increases the separation between the conduction band states $\Gamma_{3c} - \Gamma_{1c}$, from 2.37 eV in the random alloy to $\bar{\Gamma}_{1c} - \bar{\Gamma}_{1c} = 2.54$ eV in the ordered case. In spite of this 0.17 eV increase, the LDA results show only a negligible change (in fact, a slight increase) in the $E_g^{(z)}$ band gap. This can be caused by the fact that the LDA calculations significantly underestimate the band gaps, by up to 40%, which increases the across-band-gap $\bar{\Gamma}_{1c} \leftrightarrow \bar{\Gamma}_{1v}$ repulsion. Such an artificial increase in the $\bar{\Gamma}_{1c} \leftrightarrow \bar{\Gamma}_{1v}$ repulsion may suppress the effect of the $\bar{\Gamma}_{1c} \leftrightarrow \bar{\Gamma}_{1c}$ repulsion on the band gap.

(ii) *Scaling of the band gap reduction with the order parameter η* : To simulate partially ordered alloys we use a relatively large, $12 \times 12 \times 8$ primitive cells, or 4608 atoms, wurtzite supercell and occupy each cation site by Al or Ga according to Eq. (1). For a given η , we average over a set of 5 different randomly generated configurations. Since such large supercells are beyond the ability of first-principles treatment, a different, though still fully atomistic, approach is used.

The atomic positions are relaxed within the valence force field method (VFF).^{19,20} We use the traditional VFF treatment of the wurtzite structure,²¹ as in a previous wurtzite Al_xGa_{1-x}N study.²² This includes bond bending and bond stretching terms, with force constants derived from LDA calculations.²³ We do not include the long-range electrostatic terms to the VFF energy of wurtzite nitrides, studied recently in Ref. 24, as we do not use the VFF method to obtain formation energies. Instead, we use the VFF method only to optimize atomic positions, which are then used for electronic structure calculations. We find that our VFF method reproduces well the atomic positions in Al_xGa_{1-x}N alloys. For example, for the AlGa_{0.5}N₂ ordered phase the VFF (LDA) optimized bond lengths are 1.89 (1.88) Å for Al-N and 1.95 (1.94) Å for Ga-N bonds along the (0001) direction. For bonds along other directions, we obtain 1.91 (1.89) Å for Al-N and 1.93 (1.92) Å for Ga-N bonds.

The electronic structure is calculated using the recent developments in the empirical pseudopotential method (EPM),²⁵ which include local environment²⁶ and local strain²⁷ dependences. The Schrödinger equation is efficiently solved with the folded spectrum method.²⁸ We fit screened pseudopotentials for binary compounds to (i) measured principal band gaps,²⁹ (ii) LDA-calculated crystal field splittings and AlN/GaN valence band offset,³⁰ (iii) GW -calculated band energies³¹ at high symmetry points, (iv) measured band gap pressure coefficients,³² and (v) LDA calculated absolute

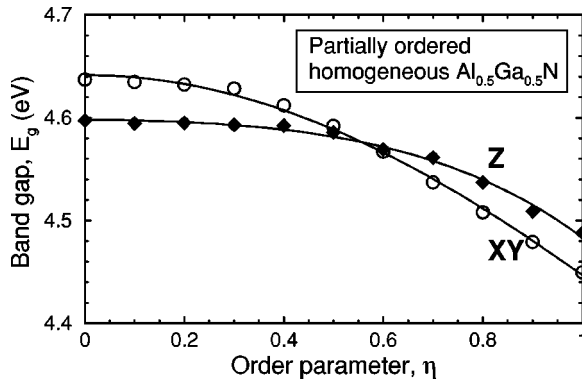


FIG. 2. Order-parameter dependence of band gap for xy -polarized (XY) and z -polarized (Z) optical transitions in $\text{Al}_{0.5}\text{Ga}_{0.5}\text{N}$, calculated using the empirical pseudopotential method. The solid lines show fits of the data points with $E_g(\eta) = a_0 + a_2\eta^2 + a_4\eta^4$ curves.

valence band volume deformation potentials³³ for a zinc blende structure. The accuracy of the fit results compared to the target values is within 0.01 eV for principal band gaps; less than 0.001 eV for the crystal field splittings and valence band offsets; within around 0.1 eV for energies of Γ_{5v} , M_{1c} , M_{4v} , $A_{1,3c}$, $A_{5,6v}$, and $L_{1,3c}$ states; within 2% for Γ_{3c} , and within a few percent for K_{2c} and H_{3c} ; within 2% for band gap pressure coefficients; and within 5% for valence band volume deformation potentials. With the present potential, a 1536-atom cell (and five configuration) calculation for random $\text{Al}_{0.5}\text{Ga}_{0.5}\text{N}$ alloy gives the band gap bowing coefficient of 1.06 eV, which is in the range 0.7–1.33 eV of recently measured values.³⁴ Our calculated effective masses are close, within around 30%, to measured electron effective masses²⁹ and non-spin-orbit LDA calculated hole effective masses,³⁵ while being systematically underestimated. The calculated band gap reductions are $\Delta E_g^{(xy)} = 0.19$ (0.17), $\Delta E_g^{(z)} = 0.11$ (−0.02), and $\Delta E_g = 0.15$ (0.09) eV, which are probably more accurate than the LDA values (in parentheses).

Figure 2 shows how the band gap of the $\text{Al}_{0.5}\text{Ga}_{0.5}\text{N}$ random alloy depends on the degree η of order. We separately show the $\bar{\Gamma}_{1v} \leftrightarrow \bar{\Gamma}_{1c}$ (z -polarized) and $\bar{\Gamma}_{3v} \leftrightarrow \bar{\Gamma}_{1c}$ (xy -polarized) gaps. Consistent with our LDA results discussed above, the $E_g^{(xy)}$ band-gap reduction at full ordering is noticeably larger than the corresponding $E_g^{(z)}$ band-gap reduction, and the lowest-energy transition is z -polarized for the random alloy and xy -polarized for the ordered one, as explained above. Figure 2 also shows that the change from the z - to xy -polarized lowest-energy gap occurs at $\eta = 0.56$, which is the crossing point of the $E_g^{(xy)}(\eta)$ and $E_g^{(z)}(\eta)$ curves.

A general theoretical analysis¹¹ proves that the band gap dependence on the long-range order parameter η should be a sum of even powers of η , with a leading term η^2 and possibly one or few non-negligible higher order corrections ($\sim \eta^4, \eta^6, \dots$). As demonstrated in Fig. 2, our calculated $E_g^{(xy)}$ and $E_g^{(z)}$ values for different degrees of order η are fit well with $a_0 + a_2\eta^2 + a_4\eta^4$ curves (solid lines). Here the fit coefficients are $a_0 = 4.642$, $a_2 = -0.217$, and $a_4 = 0.023$ eV

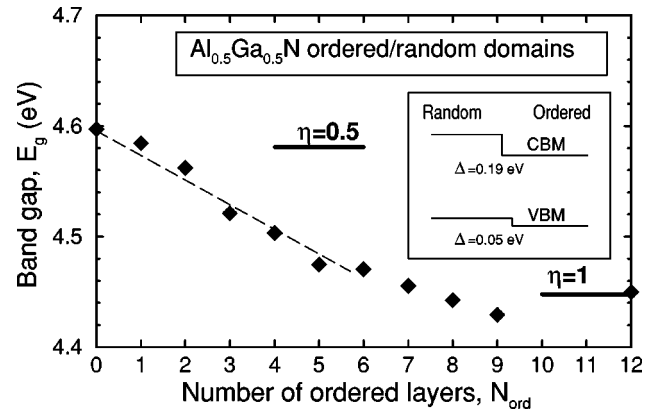


FIG. 3. Band gap reduction for ordered domains in a random matrix. EPM-calculated band gaps for systems of N_{ord} -layer thick perfectly ordered domains separated by $(12 - N_{\text{ord}})$ -layer thick regions of perfectly random alloy, simulated in a $12 \times 12 \times 12$ (6912 atoms) supercell. The insert shows a type II band alignment between perfectly ordered and random alloys.

for $E_g^{(xy)}(\eta)$ and $a_0 = 4.598$, $a_2 = -0.050$, and $a_4 = -0.064$ eV for $E_g^{(z)}(\eta)$. From Fig. 2 we see that if one assumes a homogeneous partially ordered alloy, the band gap reduction is rather small. For $\eta \sim 0.3$ – 0.6 it is less than 0.03 eV, much smaller than the observed^{8–10} redshifts of more than 0.1 eV. To understand this discrepancy, we next consider *inhomogeneously ordered* alloys.

(iii) *Coexistence of ordered and disordered domains*: Molecular beam epitaxy grown partially ordered $\text{Al}_x\text{Ga}_{1-x}\text{N}$ and $\text{In}_x\text{Ga}_{1-x}\text{N}$ layers are often found to consist of ordered-alloy domains embedded in random-alloy matrix,^{36,37} so that measured order parameter could represent an average over a number of ordered and random domains.¹⁰ To model such a situation, we consider a system of (0001)-oriented N_{ord} -layer thick slabs of perfectly ordered AlGaIn_2 ($\eta = 1$) embedded

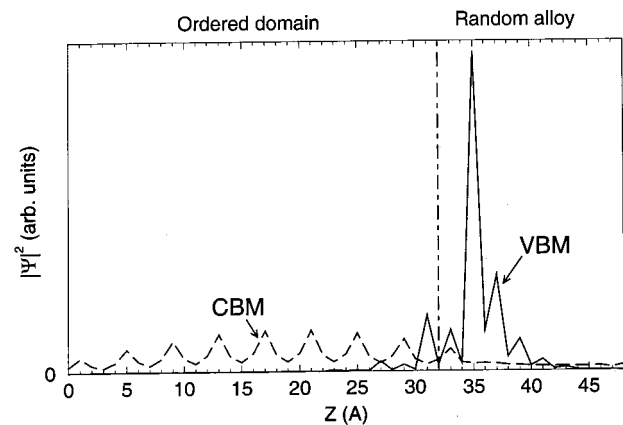


FIG. 4. Spatial distribution of the xy -averaged wave function amplitude squared ($|\psi|^2$) for the conduction band maximum (CBM) and valence band minimum (VBM) along the z axis of the supercell (Z), containing 9 ordered and 3 random layers (corresponds to $N_{\text{ord}} = 9$ in Fig. 3). Note that the CBM state is localized on the ordered domain, whereas the VBM one is localized on the random domain.

in $(12 - N_{\text{ord}})$ -layer thick random-alloy slabs ($\eta=0$). We use a $12 \times 12 \times 12$ supercell, consisting of 6912 atoms, averaging over three configurations. The averaged order parameter over supercell is defined as $\bar{\eta} = N_{\text{ord}}/12$. Remarkably, already at $N_{\text{ord}}=4-7$ ($\bar{\eta}=0.33-0.58$) the calculated band gap reduction (Fig. 3) is as large as 0.1–0.15 eV, approaching the maximal band gap reduction value of $\Delta E_g(1) = 0.15$ eV. Thus, the existence of ordered and random domains can explain the observation of >0.1 eV band gap reductions for *partially* ordered, $\eta=0.3-0.6$, alloys, even though their values are close to $\Delta E_g(\eta=1)$. The η^2 and η^4 scaling laws of homogeneous ordering are not applicable in this case; thus simple extrapolations from $\eta=0.3-0.6$ to $\eta=1$ are unjustified.

The insert in Fig. 3 shows that our predicted band alignment between ordered and disordered domains is type II. Thus, if carriers can transport through the different domains, electrons will be localized in the ordered domains, whereas the holes will be in the random alloy part (as suggested in Ref. 37), leading to a band gap reduction that can even exceed that in the maximally ordered homogeneous alloy. This is illustrated by the VBM and CBM wavefunction plots in Fig. 4. The charge separation may explain the long carrier lifetimes measured in Ref. 37.

The authors thank T. D. Moustakas, M. Albrecht, P. R. C. Kent, and C. Persson for helpful discussions. This work was supported by the U.S. Department of Energy, SC-BES-DMS Grant No. DEAC36-98-GO10337.

- ¹A. Zunger and S. Mahajan, in *Handbook of Semiconductors*, 2nd ed., edited by S. Mahajan (Elsevier, Amsterdam, 1994), Vol. 3, p. 1399.
- ²D. Korakakis, K.F. Ludwig, Jr., and T.D. Moustakas, *Appl. Phys. Lett.* **71**, 72 (1997).
- ³P. Ruterana, G. Nouet, W. Van der Stricht, I. Moerman, and L. Considine, *Appl. Phys. Lett.* **72**, 1742 (1998).
- ⁴P. Ruterana, G. De Saint Jores, and F. Omnes, *Mater. Sci. Eng., B* **82**, 203 (2001).
- ⁵E. Iliopoulos, K.F. Ludwig, Jr., T.D. Moustakas, and S.N.G. Chu, *Appl. Phys. Lett.* **78**, 463 (2001).
- ⁶P. Ruterana, G. De Saint Jores, M. Läugt, F. Omnes, and E. Bellet-Amalric, *Appl. Phys. Lett.* **78**, 344 (2001).
- ⁷M. Benamara, L. Kirste, M. Albrecht, K.W. Benz, and H.P. Strunk, *Appl. Phys. Lett.* **82**, 547 (2003).
- ⁸D.G. Ebling, L. Kirste, K.W. Benz, N. Teofilov, K. Thonke, and R. Sauer, *J. Cryst. Growth* **227-228**, 453 (2001).
- ⁹E. Iliopoulos, T.D. Moustakas *et al.* (unpublished).
- ¹⁰M. Albrecht *et al.* (unpublished).
- ¹¹D.B. Laks, S.-H. Wei, and A. Zunger, *Phys. Rev. Lett.* **69**, 3766 (1992).
- ¹²M. Suzuki, T. Uenoyama, and A. Yanase, *Phys. Rev. B* **52**, 8132 (1995).
- ¹³C. Persson, A. Ferreira da Silva, R. Ahuja, and B. Johansson, *J. Cryst. Growth* **231**, 397 (2001).
- ¹⁴A. Zunger, S.-H. Wei, L.G. Ferreira, and J.E. Bernard, *Phys. Rev. Lett.* **65**, 353 (1990).
- ¹⁵A. van de Walle and G. Ceder, *J. Phase Equilib.* **23**, 348 (2002).
- ¹⁶W. Kohn and L.J. Sham, *Phys. Rev.* **140**, A1133 (1965); D.M. Ceperley and B.J. Alder, *Phys. Rev. Lett.* **45**, 566 (1980); J.P. Perdew and A. Zunger, *Phys. Rev. B* **23**, 5048 (1981).
- ¹⁷G. Kresse and J. Furthmüller, *Phys. Rev. B* **54**, 11 169 (1996); *Comput. Mater. Sci.* **6**, 15 (1996).
- ¹⁸G. Kresse and D. Joubert, *Phys. Rev. B* **59**, 17 958 (1999); P.E. Blöchl, *ibid.* **50**, 1758 (1994).
- ¹⁹P. Keating, *Phys. Rev.* **145**, 637 (1966).
- ²⁰J.L. Martins and A. Zunger, *Phys. Rev. B* **30**, 6217 (1984).
- ²¹R.M. Martin, *Phys. Rev. B* **6**, 4546 (1972).
- ²²T. Mattila and A. Zunger, *J. Appl. Phys.* **85**, 160 (1999).
- ²³K. Kim, W.R.L. Lambrecht, and B. Segall, *Phys. Rev. B* **53**, 16 310 (1996).
- ²⁴F. Grosse and J. Neugebauer, *Phys. Rev. B* **63**, 085207 (2001).
- ²⁵K. Kim, P.R.C. Kent, A. Zunger, and C.B. Geller, *Phys. Rev. B* **66**, 045208 (2002).
- ²⁶K.A. Mader and A. Zunger, *Phys. Rev. B* **50**, 17 393 (1994).
- ²⁷L.-W. Wang, J. Kim, and A. Zunger, *Phys. Rev. B* **59**, 5678 (1999).
- ²⁸L.-W. Wang and A. Zunger, *J. Chem. Phys.* **100**, 2394 (1994).
- ²⁹I. Vurgaftman, J.R. Meyer, and L.R. Ram-Mohan, *J. Appl. Phys.* **89**, 5815 (2001).
- ³⁰S.-H. Wei and A. Zunger, *Appl. Phys. Lett.* **69**, 2719 (1996).
- ³¹A. Rubio, J.L. Corkill, M.L. Cohen, E.L. Shirley, and S.G. Louie, *Phys. Rev. B* **48**, 11 810 (1993); To correct GW band gap of AlN, a 0.4 eV upward conduction-band shift is applied.
- ³²W. Shan, J.W. Ager III, W. Walukiewicz, E.E. Haller, B.D. Little, J.J. Song, M. Schurman, Z.C. Feng, R.A. Stall, and B. Goldenberg, *Appl. Phys. Lett.* **72**, 2274 (1999).
- ³³S.-H. Wei and A. Zunger, *Phys. Rev. B* **60**, 5404 (1999).
- ³⁴W. Shan, J.W. Ager III, K.M. Yu, W. Walukiewicz, E.E. Haller, M.C. Martin, W.R. McKinney, and W. Yang, *J. Appl. Phys.* **85**, 8505 (1999); F. Yun, M.A. Reshchikov, L. He, T. King, H. Markoc, S.W. Novak, and L. Wei, *ibid.* **92**, 4837 (2002); Q.S. Paduano, D.W. Weyburne, L.O. Bouthillette, S.Q. Wang, and M.N. Alexander, *Jpn. J. Appl. Phys.* **41**, 1936 (2002).
- ³⁵K. Kim, W.R.L. Lambrecht, B. Segall, and M. van Schilfhaarde, *Phys. Rev. B* **56**, 7363 (1997).
- ³⁶D. Doppalapudi, S.N. Basu, and T.D. Moustakas, *J. Appl. Phys.* **85**, 883 (1999).
- ³⁷M. Misra, D. Korakakis, H.M. Ng, and T.D. Moustakas, *Appl. Phys. Lett.* **74**, 2203 (1999).